Front. Earth Sci. 2019, 13(1): 43–54
https://doi.org/10.1007/s11707-018-0706-z

RESEARCH ARTICLE

Assessing the relative role of climate change and human activities in desertification of North China from 1981 to 2010

Duanyang XU (✉)[1], Alin SONG[2], Dajing LI[1], Xue DING[3], Ziyu WANG[4]

1 Institute of Geographic Sciences and Natural Resources Research, Chinese Academy of Sciences, Beijing 100101, China
2 Institute of Agricultural Resources and Regional Planning of Chinese Academy of Agricultural Sciences, Beijing 100081, China
3 College of Resources and Environment, Northeast Agricultural University, Harbin 150030, China
4 College of Forestry, Beijing Forestry University, Beijing 100083, China

Abstract Desertification is a severe environmental problem induced by both climate change and human activities. This study assessed the relative contribution of climate change, human activities, and different climatic and anthropogenic factors in desertification reversion and expansion of North China from 1981 to 2010. The results showed that the desertification of North China had changed significantly over the past 30 years; desertification reversion and expansion covered an area of 750,464 km^2, and the spatial distribution of these regions exhibited considerable heterogeneity. For desertification reversion, climate change and human activity accounted for 22.6% and 26%, respectively of total reverted land. Wind speed reduction and the improvement of hydrothermal conditions were the most important climatic factors for desertification reversion in the arid region of Northwest China (ARNC) and the Three-River Headwaters region (TRHR), and the reduction in grassland use intensity was the most important anthropogenic factor related to desertification reversion in Inner Mongolia and regions along the Great Wall (IMGW). For desertification expansion, the relative role of climate change was more obvious, which was mainly attributed to the continuous reduction in precipitation in eastern IMGW, and the increase in grassland use intensity was the main factor underlying regional human-induced desertification expansion.

Keywords desertification, climate change, human activity, relative role, North China

Received October 28, 2017; accepted February 25, 2018

E-mail: xudy@igsnrr.ac.cn

1 Introduction

Desertification is defined as land degradation in arid, semi-arid, and dry sub-humid areas resulting from various factors including climatic variations and human activities (UNCCD, 1994). China is one of the countries which is seriously affected by desertification. According to the fifth desertification survey statistics of the State Forestry Administration, the desertified area in China reached 2,611,600 km^2 in 2014, which accounted for 27.20% of the country's total land area (State Forestry Administration of China, 2015). The problems induced by land desertification, such as soil quality decline, loss of biodiversity, and sand storms, etc., have seriously restricted the development of the economy and society, as well as the health of the Chinese people (Wang et al., 2013; Wang, 2014; Tang et al., 2015). Previous research showed that the indirect economic loss caused by desertification in 10 provinces of North China could reach 48.79 billion CNY (Ma et al., 2008).

In order to control desertification, the Chinese Government has implemented the Three-North Shelterbelt Project, Beijing-Tianjin Sandstorm Source Treatment Project, Grain for Green Project, no grazing policy, and other ecological protection projects and policies since the 1970s, which have played a positive role in desertification reversion (Zhang et al., 2012; Wu et al., 2013; Tan and Li, 2015; Xie et al., 2015). Meanwhile, rapid urbanization, combined with the over-exploitation of mineral resources and irrational land use behaviors, have made many regions in the ecological fragile areas of North China experience desertification expansion (Yan and Hua, 2011; Ge et al., 2016; Liu et al., 2016). The impact of climate change on desertification is directly reflected by the effect of interannual variability in rainfall, temperature, wind speed, and other climatic factors on vegetation-soil system

succession (Sivakumar, 2007; Wang et al., 2016, 2017). In recent decades, the warming climate in North China intensified the risk of land desertification (Chen and Tang, 2005), but other studies showed that the weakening of wind erosion in North China over the past few decades was an important factor leading to desertification reversion, and the relative role of the ecological protection projects was overestimated (Wang et al., 2010). Climate change and human activities have considerable spatial heterogeneity, and their interaction with different vegetation-soil systems that lead to land desertification reversion and expansion in North China also has obvious temporal-spatial heterogeneity (Peters and Havstad, 2006; Wang, 2014; Chen and Wang, 2016).

To deeply understand the evolution process and mechanism of desertification, it is urgent to identify, separate and evaluate the relative role of climate change and human activities in desertification reversion and expansion (Peters and Havstad, 2006; Wang, 2014; Chen and Wang, 2016). In recent years, numerous methods have been developed to quantitatively separate and assess the relative role of climate change and human activities in desertification, such as the Principal Component Analysis method (Li et al., 2007; Ma et al., 2007), Rain Use Efficiency (RUE) method (Prince et al., 1998, 2007; Holm et al., 2003), RESTREND (Residual Trends) method (Evans and Geerken, 2004; Geerken and Ilaiwi, 2004; Wessels et al., 2004, 2007; Xu et al., 2014), LNS (Local NPP Scaling) method (Wessels et al., 2008; Prince et al., 2009), and so on. Comparatively, the RUE and RESTREND methods are based on the long time series of land surface vegetation information, such as the Normalized Difference Vegetation Index, NDVI, and Net Primary Productivity, NPP, having the advantages of separating and quantifying the relative role of climate change and human activities in desertification and being suitable for different spatial and temporal scales. In addition, the RESTREND method is a helpful tool that can effectively identify human-induced degradation, combined with the theoretical trend of NDVI (forecasting NDVI by using a regression model and rainfall data) or potential NPP to evaluate the relative roles of climate change and human activities (Vu et al., 2014; Xu et al., 2014; Zhou et al., 2015).

However, due to the difficulty and uncertainty in retrieving the key parameters at large scales, especially desertification data at national scales and multiple temporal scales, the results of current research cannot be used to assess the relative role of climate change and human activities in the desertification of North China over the past 30 years. Meanwhile, previous studies paid less attention to separate the roles of different climatic and anthropogenic factors (Xu et al., 2014; Zhou et al., 2015; Li et al., 2016), which makes it very difficult to successfully explain the driving force of desertification at different scales. Therefore, based on the identification of desertification dynamics in North China from 1981 to 2010, this study aims to (i) assess the relative role of climate change and human activities in desertification reversion and expansion over the past 30 years, and (ii) identify the effects of different climate factors, land use pattern, and land use intensity on desertification reversion and expansion.

2 Materials and methods

2.1 Study area

Desertification in North China mainly occurs in Inner Mongolia, Ningxia, Gansu, Xinjiang, Qinghai, Shaanxi, Shanxi, Hebei, and other provinces. The whole study area covers approximately 4000 km from east to west, and the area spans 3,022,848 km^2. The climatic characteristics of this region exhibit great spatial heterogeneity. Precipitation ranges between 0 and 450 mm, the average temperature is approximately 5.7°C, the average annual sunshine duration is 2807 hours, and the average wind speed reaches 2.3 m/s. Most of the soil in this area is chestnut soil, brown soil, brown desert soil, mattic soil, and sandy soil. In order to facilitate statistical and comparative analyses, the study area was divided into three sandy areas according to the climate characteristics and natural geographical environment (Wang, 2004): Inner Mongolia and regions along the Great Wall (IMGW), the arid region of Northwest China (ARNC) and the Three-River Headwaters region (TRHR). Due to the large areas of IMGW and TRHR, they were divided into 9 and 10 sub-regions (Fig. 1), respectively. IMGW includes the Hulun Buir grassland (hlbr), Horqin grassland (horq), Hunshandake sandy land (hsdk), Chahar grassland (char), Bashang area (bash), Wumeng Qianshan and Tumote plain (wmt), the northwest of Shanxi Province (jxb), Erdos grassland (erdos), and Ningxia Hedong sandy land (nxhd). ARNC includes the Chaidamu basin (cdm), Alashan plateau (alsh), Hetao plain (htpy), Hexi Corridor (hxzl), Houshan region in Inner Mongolia (nmhs), Tarim basin (talm), Turpan Hami basin (thpd), Yinchuan plain (ycpy), Yili basin (ylpd) and Zhungeer basin (zhgr).

2.2 Data collection and processing

The data used in this study include remote sensing images, climate, soil, vegetation, land use and socio-economic statistics, etc. Landsat MSS/TM/ETM + images covering the research region in the 1980s and 2010s were obtained from the United States Geological Survey (USGS), which were used to monitor the desertification dynamics; all images were radiometrically and geometrically corrected. Maximum Value Composites (MVC) NDVI data (8 km resolution and 15-day) from 1981 to 2006 were obtained from the Global Inventor Modeling and Mapping Studies (GIMMS) of the National Aeronautics and Space Administration (NASA); 1 km resolution and 16-day composited

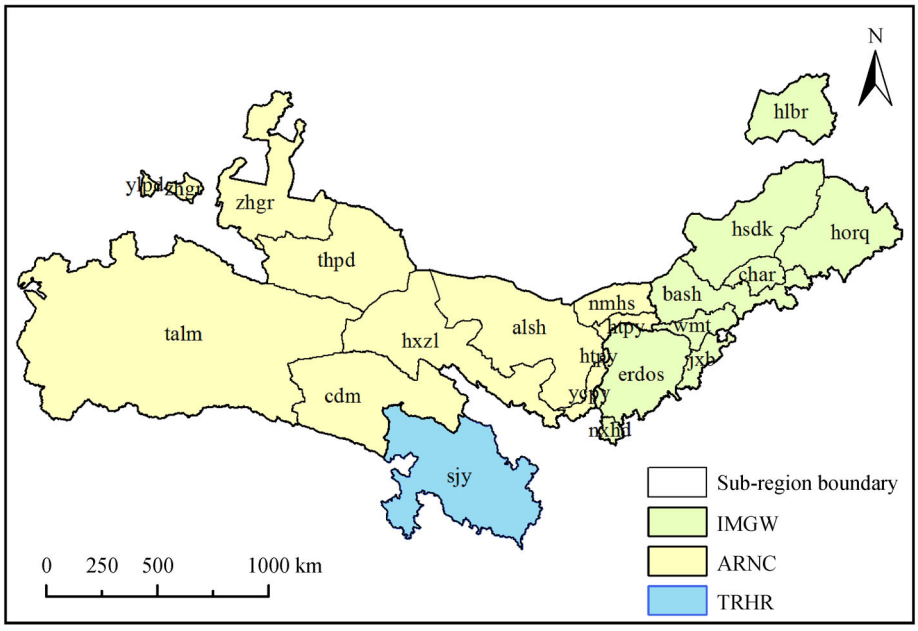

Fig. 1 The location of study area.

MODIS NDVI data (MOD13A1) from 2001 to 2010 were retrieved from the USGS. In order to construct the homogeneous NDVI time series from 1981 to 2010, 2007–2010 MODIS NDVI data were converted to GIMMS NDVI data by using regression models at a monthly scale, which were established by overlapping two datasets from 2001–2006. Climate data (e.g., precipitation, temperature, sunshine duration, and wind speed) for 1981–2010, recorded by meteorological stations in the research region, were obtained from the National Meteorological Information Center. 1:1,000,000 Chinese soil and vegetation maps, 1:100,000 Chinese desert map, and land use data (1-km resolution) from the 1980s to 2010s were adopted from the Chinese Academy of Sciences Resource Environmental Data Center. Population, livestock, and afforestation area data were derived from Statistical Yearbooks of the related provinces that were included in this study, such as the Inner Mongolia Statistical Yearbook. In order to facilitate spatial analysis and comparison, NDVI data, land use data, meteorological data and vector data (e.g., vegetation and soil characteristics) used in this study were resampled, interpolated or converted to grid data with an 8-km resolution.

2.3 Methods

2.3.1 Desertification monitoring

According to previous studies and the spatial scale in this study (Wang et al., 2004), the desertified lands in North China have been classified into four grades: none, low, medium and severe desertification. Vegetation coverage (VC) was selected as an indicator to monitor the desertification degree by combining a decision tree model and supervised classification method. The method of retrieving VC was constructed by calculating the relative ratio of the real NDVI to the maximum and minimum NDVI (Eq. (1)), which is a classical method that has been validated by previous studies and the authors' field investigation (Xu et al., 2009). The specific steps of desertification monitoring are listed as follows: 1) Extract non-desertified land. According to the 1:100,000 Chinese desert map, we selected $VC \leqslant 0.02$ (glaciers, rivers, lakes, desert) and $VC \geqslant 0.6$ (dense and sparse forest, farmland, and high coverage grassland) as the criteria to extract non-desertified land; 2) Extract desertified land with other grades. For the regions with $0.02 < VC < 0.6$, low, medium, and severe desertified land, and other non-degraded grasslands and urban regions were identified by using a supervised classification method based on Landsat images and considering the differences in regions and seasons; 3) Correction and accuracy evaluation. The obtained monitoring results were overlaid on the Landsat images, and visual inspection was conducted to correct the classification errors according to the image characteristics and expert knowledge; 25 checking points for each sub-region and a total of 500 checking points for the whole research region were randomly selected to verify the results.

$$VC = \frac{NDVI - NDVI_{min}}{NDVI_{max} - NDVI_{min}}, \quad (1)$$

where VC is the vegetation coverage; NDVI is the average value of the initial three years in the 1980s (1981–1983) and the final three years in the 2010s (2008–2010). $NDVI_{min}$ is the NDVI of bare soil; and $NDVI_{max}$ is the maximum NDVI of farmland or forest.

2.3.2 Assessment of the relative role of climate change and human activities

According to previous studies (Prince, 2002; Xu et al., 2014, 2016), NPP was selected as the indicator to measure the impact of climate change and human activities on desertification. The changing trend of potential NPP (PNPP) was used to assess the relative role of climate change, and the difference between potential and actual NPP (HNPP) was used to assess the relative role of human activities. Combining the desertification reversion and expansion data with the changing trends of PNPP (SlopePNPP) and HNPP (SlopeHNPP), a scenario analysis method was developed to assess the relative role of climate change and human activities (Table 1). Take desertification reversion as an example, if PNPP had a significantly ($p < 0.1$) positive trend and HNPP did not have a significantly negative trend, this meant that climate change dominated desertification reversion.

In this study, a classical NPP model, the Carnegie–Ames–Stanford-Approach (CASA) model, was used to calculate actual NPP (Field et al., 1995; Lobell et al., 2003; Tao et al., 2005). This is a semi-process model based on remote sensing data and includes the product of absorbed photosynthetically active radiation and light-use efficiency (Eqs. (2)–(4)). The CASA model was tested and proved useful in our previous study (Xu et al., 2009). A natural vegetation NPP model (Eqs. (5) and (6)) that considers climate-vegetation characteristics and water-heat balance was adopted to calculate potential NPP, which has proven to be suitable in arid and semi-arid regions of China (Zhou and Zhang, 1995, 1996; Zhou et al., 1998).

$$\mathrm{NPP} = \mathrm{APAR} \times \varepsilon, \tag{2}$$

$$\mathrm{APAR} = \mathrm{SOL} \times \mathrm{FPAR} \times 0.5, \tag{3}$$

$$\varepsilon = T_{\varepsilon 1} \times T_{\varepsilon 2} \times W_{\varepsilon} \times \varepsilon_{\max}, \tag{4}$$

$$\mathrm{PNPP} = \mathrm{RDI}^2 \times \frac{r(1 + \mathrm{RDI} + \mathrm{RDI}^2)}{(1 + \mathrm{RDI})(1 + \mathrm{RDI}^2)} \times \exp\left(-\sqrt{9.87 + 6.25\mathrm{RDI}}\right) \times 45, \tag{5}$$

$$\mathrm{RDI} = (0.629 + 0.237\mathrm{PER} - 0.00313\mathrm{PER}^2)^2, \tag{6}$$

where NPP is actual NPP ($gC \cdot m^{-2} \cdot yr^{-1}$); APAR is absorbed photosynthetically active radiation; ε is light use efficiency; SOL is the total solar radiation (MJ $\cdot m^{-2} \cdot mo^{-1}$); FPAR is the fraction of photosynthetically active radiation that is absorbed by vegetation; $T_{\varepsilon 1}$, $T_{\varepsilon 2}$ is the limited factor of light use efficiency induced by low and high temperature, respectively; W_{ε} is the limited factor of light use efficiency induced by drought, and $\varepsilon_{\max}$ is the maximum value of light use efficiency under the condition with no limitation. PNPP is potential NPP ($gC \cdot m^{-2} \cdot yr^{-1}$); RDI is the radiation dryness index, which is determined by PER (the ratio of potential evaporation to rainfall); and r is yearly rainfall (mm).

2.3.3 Assessment of the impact of climate factors

In this study, the impacts of rainfall, temperature, sunshine duration, and average wind speed on desertification were assessed. The specific methods are described as follows: 1) Trend analysis. A linear slope ($p < 0.1$) was used to identify the climate indicators that changed significantly from 1981 to 2010. 2) Correlation analysis. A correlation between climate factors and NPP was calculated to assess whether these factors had a significant impact on desertification ($p < 0.1$). 3) Scenario analysis. Based on the above, the roles of climate factors in desertification reversion and expansion were assessed by using the scenario analysis method. For example, for a grid that experienced desertification reversion induced by climate change, if one climate factor had a significantly increasing trend and obviously positive correlation with NPP, it meant that this factor contributed significantly to desertification reversion. The assessment sketch map is shown below (Fig. 2).

Table 1 Scenario analysis table for assessing the relative role of climate change and human activities in desertification reversion and expansion

Item	SlopeCNPP	SlopeHNPP	Explanation
Desertification reversion	>0	>0	Climate change induced desertification reversion
	<0	<0	Human activities induced desertification reversion
	>0	<0	Both climate change and human activities induced desertification reversion
Desertification expansion	<0	<0	Climate change induced desertification expansion
	>0	>0	Human activities induced desertification expansion
	<0	>0	Both climate change and human activities induced desertification expansion

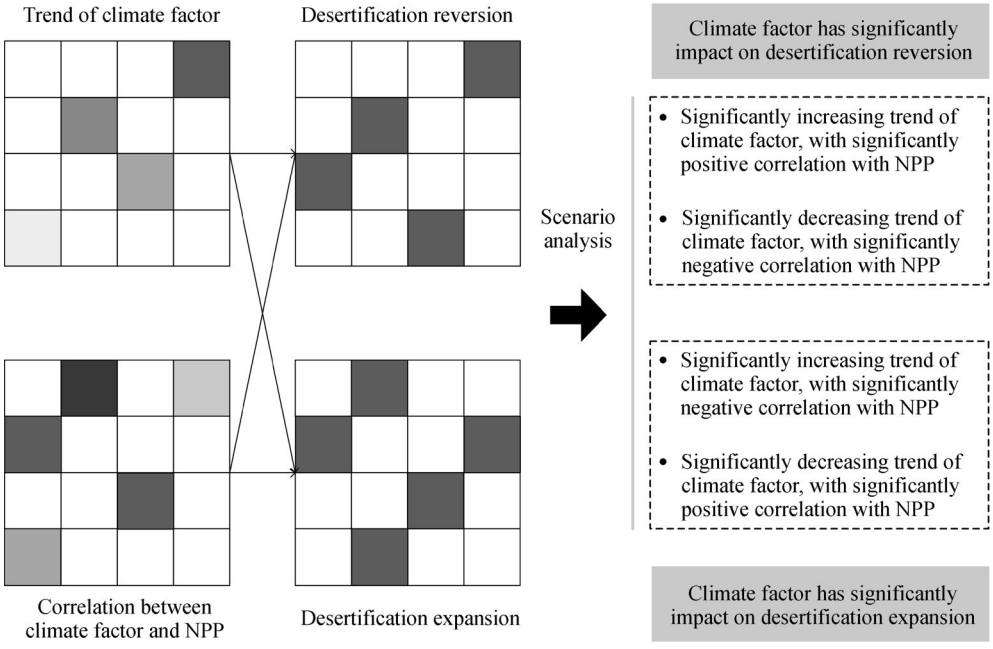

Fig. 2 The sketch map for assessing the impacts of climatic factors.

2.3.4 Assessment of the impact of land use pattern and intensity

In this study, land use pattern and intensity were selected as two indicators to assess the impact of human activities. The land use types were divided into six types: farmland, forest, grassland, urban and industrial land, unused land and water bodies. For the assessment of land use pattern, areas that were converted from unused land to farmland, forest, grassland, urban and industrial land were treated as potential desertification reversion caused by land use patterns. On the contrary, areas that converted to unused land were treated as potential desertification expansion caused by land use patterns. By overlaying these potential areas with desertification reversion and expansion induced by human activities, the impacts of land use patterns were identified. For the assessment of land use intensity, only desertification reversion and expansion caused by human activities that occurred on unchanged land use types (farmland, forest, grassland and unused land) over the past 30 years can be attributed to the impact of land use intensity.

3 Results

3.1 Desertification dynamics in North China from 1981 to 2010

According to the accuracy assessment result, the overall classification accuracy for desertification monitoring was higher than 85%. The desertification monitoring results showed that the total area of desertified land in North China did not change significantly from 1981 to 2010 and only decreased slightly from 3,018,752 km^2 to 3,015,808 km^2. However, desertified land of different grades underwent an obvious change in the past 30 years. According to the transition matrix of different desertification grades (Table 2), the total area of desertified land that experienced a grade change was 750,464 km^2, and the reversion and expansion regions accounted for 45% and 55%, respectively. With respect to desertification reversion, the area that experienced a single grade reversion accounted for 83.70% of the total reverted area. For example, 5.90% of severely desertified land was reversed to medium desertification, and 23.40% of medium desertified land was reversed to low desertification. At a sandy-area scale (Table 3), only TRHR experienced net desertification reversion, and the reverted area accounted for 87.29% of total grade-changed areas. At the sub-region level, hlbr, wmt, and nxhd of IMWG, and ycpy and zhgr of ARNC experienced net desertification reversion overall.

With respect to desertification expansion, areas that experienced a single grade expansion dominated, with 18.91% non-desertification, 17.83% low desertification and 18.78% medium desertification areas converted into low, medium and severe desertification areas, respectively. At a sandy-area scale, IMGW and ARNC experienced net desertification expansion, whereas the situation was more serious for ARNC, where the expanded area accounted for 61.34% of the whole region. At the sub-region level (Table 3), talm and hxzl of ARNC experienced obvious desertification expansion and bash and horq of IMGW also experienced desertification expansion.

Table 2 Transfer matrix of desertification grades between 1981 and 2010

1981	2010							
	Non		Low		Medium		Severe	
	Area/km^2	Percent/%	Area/km^2	Percent/%	Area/km^2	Percent/%	Area/km^2	Percent/%
Non	457,984	75.81	114,240	18.91	16,000	2.65	15,872	2.63
Low	102,016	17.20	301,568	50.84	105,792	17.83	83,840	14.13
Medium	17,472	4.12	99,136	23.40	227,456	53.69	79,552	18.78
Severe	17,280	1.25	20,864	1.50	81,856	5.90	1,266,944	91.35

Table 3 Desertification dynamics from 1981 to 2010 in north China

Region		Reversion		Expansion		No change	
		Area/km^2	Percent/%	Area/km^2	Percent/%	Area/km^2	Percent/%
Sandy area	IMGW	122,176	17.12	168,640	23.63	422,976	59.26
	ARNC	151,232	7.42	236,800	11.62	1,649,920	80.96
	TRHR	64,192	25.42	9344	3.70	178,944	70.87
Sub-region	hlbr	29,184	35.57	8192	9.98	44,672	54.45
	horq	17,984	14.06	33,536	26.21	76,416	59.73
	hsdk	27,776	14.80	41,664	22.20	118,272	63.01
	char	5184	18.45	8960	31.89	13,952	49.66
	bash	6080	6.23	32,640	33.42	58,944	60.35
	wmt	4672	21.73	3072	14.29	13,760	63.99
	jxb	6464	25.19	4224	16.46	14,976	58.35
	erdos	16,256	12.48	35,392	27.16	78,656	60.36
	nxhd	8576	66.67	960	7.46	3328	25.87
	cdm	15,872	7.11	24,960	11.18	182,336	81.70
	htpy	4992	29.66	1472	8.75	10,368	61.60
	hxzl	36,864	14.94	59,392	24.07	150,528	61.00
	nmhs	3776	8.29	6592	14.47	35,200	77.25
	talm	32,448	3.74	91,072	10.49	744,640	85.77
	thpd	7680	3.76	28,224	13.82	168,320	82.42
	ycpy	2432	15.02	384	2.37	13,376	82.61
	ylpd	384	7.69	1152	23.08	3456	69.23
	zhgr	34,176	19.61	16,512	9.47	123,584	70.91
	alsh	12,608	5.30	7040	2.96	218,112	91.74

3.2 The relative role of climate change and human activities in desertification

According to Table 1, the relative role of climate change and human activities in desertification reversion and expansion can be assessed separately (Fig. 3). From 1981 to 2010, the area of desertification reversion dominated by climate change was 76,160 km^2, which accounted for 22.6% of the total reverted land. Climate change and human activities together explained 23.8% of total desertification reversion; however, the role of climate change was relatively weak, and the reverted area caused by climate change only accounted for 3.9% of total reverted land. The relative role of human activities was similar to that of climate change, accounting for 26% of total reverted land. In different sandy areas, climate change had a more obvious impact on desertification reversion in TRHR and ARNC, whereas the opposite was observed for IMGW, and human activities were more prominent in desertification reversion. At the sub-region scale, desertification reversion in cdm, alsh, ylpd and zhgr of ARNC was mainly caused by climate change. By contrast,

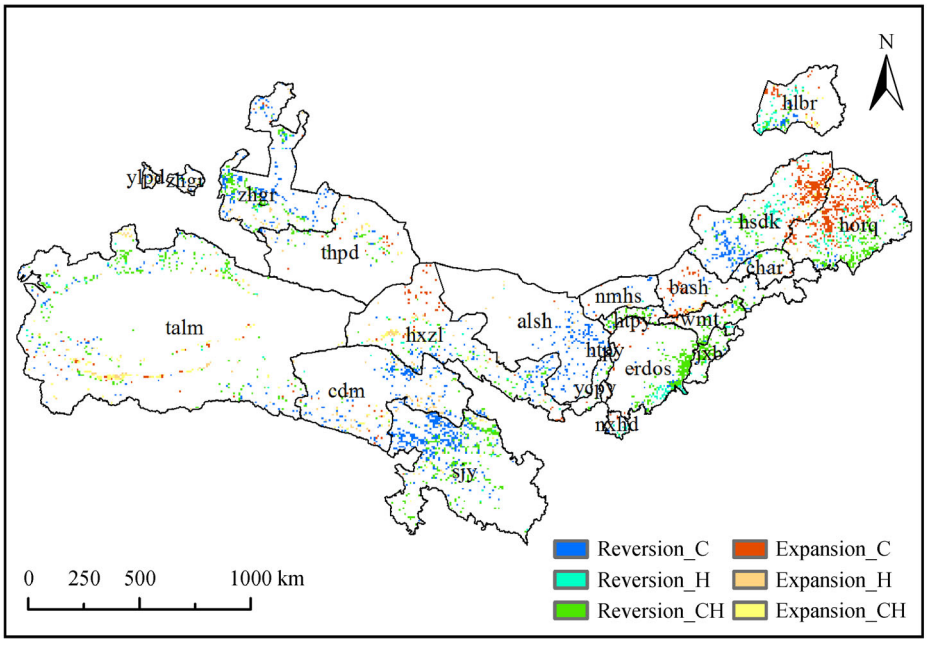

Fig. 3 The relative roles of climate change and human activities in desertification reversion and expansion of North China from 1981 to 2010 (Reversion/Expansion_C/H/CH mean climate change, human activities and both of them induced desertification reversion and expansion).

desertification reversion in erods, horq, and wtm of IMWG was mainly caused by human activities.

With respect to desertification expansion, the expanded area caused by climate change was 52,095 km^2, accounting for 12.6% of the total area of desertification expansion in North China. However, expanded area caused by human activities was only 29,888 km^2, accounting for 7.2% of the total area of desertification expansion. At a sandy-area scale, climate change had a more obvious impact on desertification expansion in IMWG than in ARNC and TRHR; especially in hlbr, horq, and hsdk, where the expanded area caused by climate change accounted for more than 30% of the total sub-region, and this proportion in horq almost reached 50%. However, the spatial distribution of expanded areas caused by human activities was more scattered.

3.3 The relative role of climate factors in desertification

According to Fig. 4 and Fig. 5, the climate factors played different roles in the processes of desertification reversion and expansion. With respect to desertification reversion, sunshine duration, average wind speed, and their combined effect were the main drivers of desertification reversion in IMGW, and the area of desertification reversion induced by these factors accounted for 73.91% of the total reverted land in IMGW. For example, the average wind speed in IMGW decreased from 3.20 m/s in the 1980s to 2.6 m/s in the 2010s, and the improvement of the wind erosion environment accelerated the stabilization of sand dunes. In ARNC (referring mainly to the southern margin of zhgr and talm) and TRHR, the improvement of hydrothermal conditions and their coupling with lower wind speed were the main climatic drivers of regional desertification reversion, and the reverted area induced by these factors accounted for more than 75% of the total reverted land in ARNC and TRHR. Taking zhgr as an example, from the 1980s to 2010s, the average rainfall and temperature increased 12.5% and 29.1%, respectively; and the average wind speed decreased by 12.5% during the same period. The relative role of climate factors in desertification reversion was relatively simple, which was mainly attributed to the decrease in regional rainfall, especially in horq and hsdk in IMGW. For example, the average rainfall of horq decreased from 450 mm in the 1980s to 340 mm in the 2010s.

3.4 The relative role of land use pattern and intensity in desertification

Based on the land use change data from 1981 to 2010 and desertification dynamics induced by human activities, the relative role of land use pattern and intensity in desertification reversion and expansion was analyzed (Table 4). With respect to desertification reversion, the decrease in land use intensity played an important role, and the reverted area induced by a decrease in land use intensity reached 89,088 km^2, which accounted for 88.44% of the total reverted area induced by human activities; this trend was more obvious in IMGW than in the other two

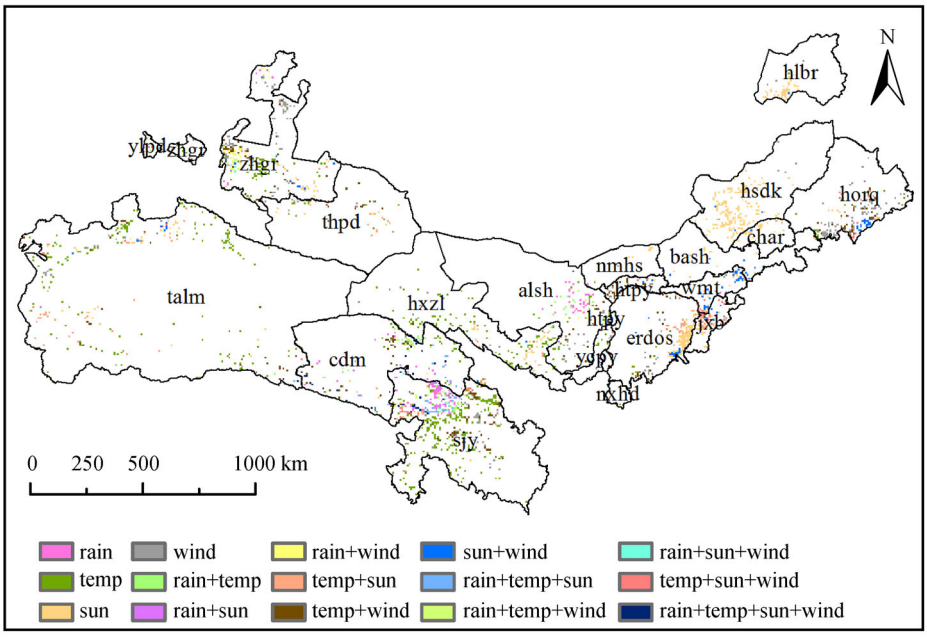

Fig. 4 The impacts of different climatic factors on desertification reversion of North China from 1981 to 2010.

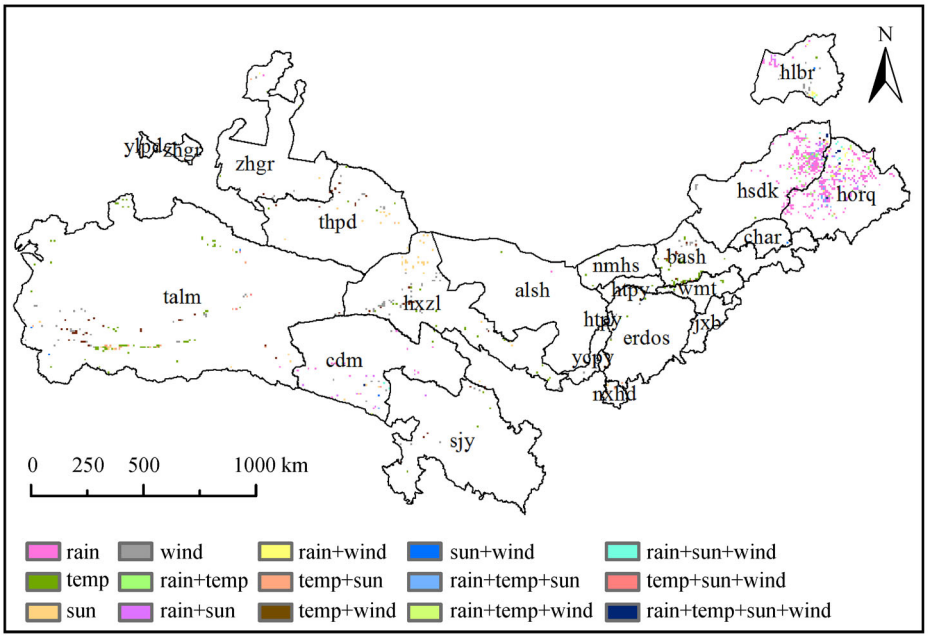

Fig. 5 The impacts of different anthropogenic factors on desertification expansion of North China from 1981 to 2010.

regions. Among different land use types, desertification reversion caused by a decrease in grassland use intensity dominated and accounted for 62.50%, 42.69%, and 81.76% of the total reverted area induced by human activities in IMGW, ARNC, and TRHR, respectively. Desertification reversion caused by the change in land use pattern accounted for 11.56% of the total reverted area induced by human activities. The regions transformed from unused land to grassland played the most important role; these areas reached 7360 km^2, accounting for 63.19% of the total reverted area induced by the change in land use pattern.

The increase in land use intensity was the main cause of human-induced desertification expansion; the area of which reached 27,520 km^2, accounting for 80.22% of the total expanded area induced by human activities, and this

Table 4 Relative role of land use pattern (LUP) and intensity (LUI) in human-induced desertification reversion and expansion

Item	Land use	IMGW		ARNC		TRHR	
		Area/km^2	Percent/%	Area/km^2	Percent/%	Area/km^2	Percent/%
LUP-Reversion		2688	23.08	7232	62.09	1728	14.84
	Farmland	704	26.19	2176	30.09	64	3.70
	Forest	192	7.14	704	9.73	128	7.41
	Grassland	1728	64.29	4096	56.64	1536	88.89
	Urban and Industrial Land	64	2.38	256	3.54	0	0.00
	Lui-Reversion	46,848	52.59	29,632	33.26	12,608	14.15
	Farmland	8832	31.36	3584	21.54	128	1.35
	Forest	576	2.05	192	1.15	128	1.35
	Grassland	17,600	62.50	7104	42.69	7744	81.76
	Unused Land	1152	4.09	5760	34.62	1472	15.54
LUP-Expansion		512	7.55	5952	87.74	320	4.72
	Farmland	0	0.00	896	15.05	64	20.00
	Forest	0	0.00	576	9.68	0	0.00
	Grassland	512	100.00	4416	74.19	256	80.00
	Urban And Industrial Land	0	0.00	64	1.08	0	0.00
	Lui-Expansion	5376	19.53	20,224	73.49	1920	6.98
	Farmland	0	0.00	128	0.91	0	0.00
	Forest	128	3.78	192	1.36	0	0.00
	Grassland	3200	94.34	6400	45.54	576	75.00
	Unused Land	64	1.89	7360	52.27	192	25.00

was more obvious in ARNC. Across different sandy areas, the increase in grassland use intensity was the main factor of human-induced desertification expansion in IMGW, and the increase in grassland and unused land use intensity dominated in ARNC and TRHR. The area of desertification expansion caused by the change in land use pattern accounted for 19.78% of the total human-induced expanded regions, and the transformation from grassland to unused land was the key factor.

4 Discussion

From 1981 to 2010, the climate and human activities in North China experienced significant changes, and the extensive heterogeneity of these changes has caused considerable differences in desertification reversion and expansion patterns in different regions (Wang, 2014; Wang et al., 2016). Although many areas experienced obvious desertification reversion over the past 30 years, desertification expansion in some regions had not been well controlled, such as the lower reaches of Tarim River (talm), which coincided with the fourth desertification survey statistics conducted by the State Forestry Administration of China (2011).

The differences of the impact of climate change on desertification dynamics were mainly reflected at large spatial scales. Take the aridity/humidity index (calculated as the ratio of rainfall to potential evapotranspiration, which is a reliable indicator to reflect climate change and its impact on land surface vegetation growth) as an example (Wu et al., 2005): this index displayed an increasing trend in ARNC and TRHR and a decreasing trend in IMGW (Fig. 6(a)), which meant that the land surfaces of ARNC and TRHR were more humid and suitable for vegetation rehabilitation and desertification reversion; this result is in agreement with the clear increasing trends of rainfall in Northwest China over the past 30 years, which have been proved by the fourth desertification survey statistics in China (State Forestry Administration of China, 2011) and previous studies (Sun et al., 2015; Zhang et al., 2016). In addition, the decreased wind speed across the whole of North China significantly improved the wind erosion environment of desertified land, and the average wind erosion index (FAO, 1979) of the study region decreased from 30.6 in the 1980s to 23.3 in the 2010s (Fig. 6(b)). The improvement of the wind erosion environment at a large scale provided a good condition for vegetation restoration and has been considered as the main factor contributing to desertification

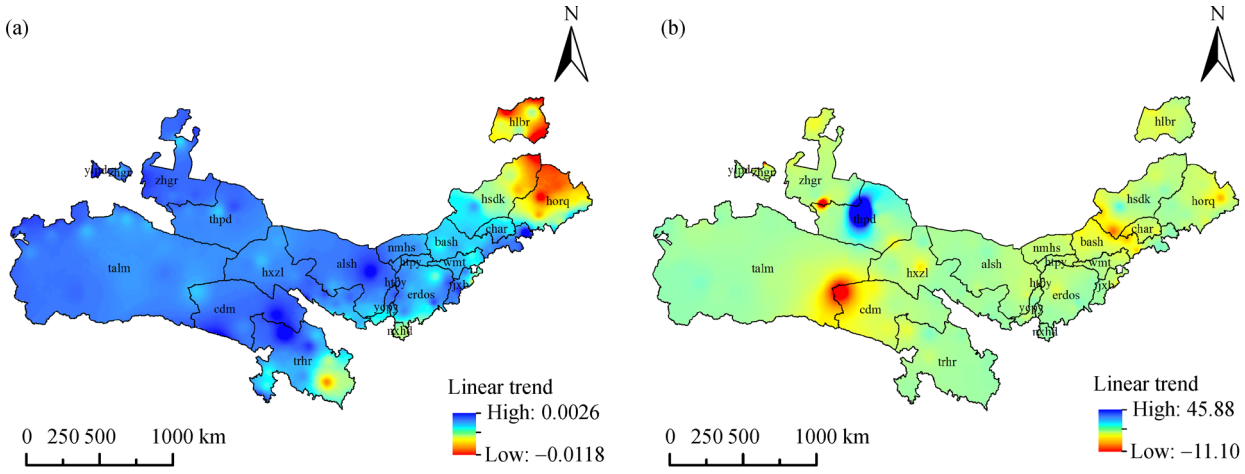

Fig. 6 The linear trend of aridity/humidity index of desertified land of North China from 1981 to 2010.

reversion (Wang et al., 2006, 2010). Overall, climate change in ARNC and TRHR was more conductive for desertification reversion compared with IMGW; however, due to regional drought, climate change played a more important role in desertification expansion in IMGW than in the two other regions.

Restricted by rural settlement, road accessibility, and regional environmental conditions, the impacts of human activities on desertification dynamics appear relatively scattered in space, concentrated mainly along the edge of the oasis in ARNC and in the middle-eastern region of IMGW, and these areas are active regions with respect to economy and land use. The reduction in grassland use intensity induced by ecological protection policies (such as no grazing policy) was the dominant anthropic factor of desertification reversion (Huang et al., 2013; Wu et al., 2013; Tan and Li, 2015; Xu et al., 2016) and was also coupled with the increasing trend of rainfall that accelerated desertification reversion, especially in ARNC and TRHR (State Forestry Administration of China, 2011). However, the impact of human activities on desertification reversion may be lower when analyzed at a 30-year scale because the ecology-environment protection policy and projects (e.g., the TRHR Treatment project) in China were not widely launched between 1981 and 2000 (Zhang et al., 2016). In addition, there were also time lag effects of the ecology-environment protection policy and projects on desertification reversion due to the recovery rate of vegetation (Tong et al., 2017), especially for those implemented after 2000, which means that positive impacts of human activities might be underestimated in this study. In addition, some areas have undergone extensive human activities, such as energy and mineral exploitation, network expansion, psammophyte excavation and so on, which would lead to desertification expansion (Hao and Ren, 2009; State Forestry Administration of China, 2011; Ge et al., 2016). Take Inner Mongolia as an example: the total energy production increased nearly 10-fold from 2000 to 2010 (Xu et al., 2014). Energy exploitation will inevitably lead to the destruction of land surface environments and the excessive use of groundwater, which is harmful to vegetation restoration in sandy areas. In addition, road expansion has been identified as an important factor that has a significant effect on vegetation degradation in Inner Mongolia, Xinjiang and other regions (Feng et al., 2015). Therefore, it is crucial to scientifically plan and guide industrial distribution and consumer behavior in ecologically fragile areas.

This study has mainly focused on the statistically significant impact of climate change and human activities on desertification at the time scale of 30 years, which might ignore the impact of some short-term sudden changes. Many uncertainties remain related to short-term extreme weather and engineering activities, which would not be detected when using the linear regression method. Besides, two sources of NDVI data were used in this study; although month-level regression models were developed to covert MODIS NDVI to GIMMS NDVI, errors remained in the consistency of the NDVI time series, which would have an impact on the accuracy of desertification monitoring and NPP estimation and would increase the uncertainty of the results. Therefore, high-resolution remote sensing images and higher spatial-temporal resolution meteorological data will be used to identify the desertification dynamics induced by short-term climate variation and human activities in future studies. Meanwhile, multiple regression models and nonparametric tests can be used to analyze the influence of different factors at the grid scale.

5 Conclusions

From 1981 to 2010, desertification in North China

underwent a significant change driven by both climate change and human activities. Generally, the area of desertification reversion was almost equivalent to desertification expansion, but the spatial distribution of these regions exhibited considerable heterogeneity. The reverted regions occurred mainly in hlbr, wmt, nxhd, zhgr, alsh, and TRHR, whereas the expanded areas occurred mainly in talm, hxzl, bash, and horq.

With respect to desertification reversion, the effects of climate change and human activities are almost equivalent, but they exhibit considerable spatial heterogeneity. For instance, climate change dominated desertification reversion in ARNC and TRHR, and reduced wind speed and the improvement of hydrothermal conditions were the most important climatic factors. However, human activities dominated desertification reversion in IMGW, which can be attributed to the reduction in grassland-use intensity induced by the implementation of ecological protection projects and policy after 2000. With respect to desertification expansion, the relative role of climate change was more obvious, which was mainly attributed to the continuous reduction in precipitation in eastern IMGW (such as in horq). Human-induced desertification expansion was relatively decentralized in space, which was mainly caused by regional high-intensity use of grasslands. In order to assess the relative roles of different driving factors at different spatial and temporal scales, high-resolution images and multiple regression models should be used in future studies.

Acknowledgements This research was jointly supported by the National Key Research and Development Program of China (No. 2016YFC0501002) and the National Natural Science Foundation of China (Grant No. 71573245).

References

Chen N, Wang X P (2016). Driver-system state interaction in regime shifts: a model study of desertification in drylands. Ecol Modell, 339: 1–6

Chen Y, Tang H (2005). Desertification in north China: background, anthropogenic impacts and failures in combating it. Land Degrad Dev, 16(4): 367–376

Evans J, Geerken R (2004). Discrimination between climate and human-induced dryland degradation. J Arid Environ, 57(4): 535–554

FAO, UNEP, UNESCO (1979). A provisional methodology for soil degradation assessment. Rome: FAO, 84pp

Feng Q, Ma H, Jiang X, Wang X, Cao S (2015). What has caused desertification in China? Sci Rep, 5(1): 15998

Field C B, Randerson J T, Malmstrom C M (1995). Global net primary production- combining ecology and remote-sensing. Remote Sens Environ, 51(1): 74–88

Ge X D, Dong K K, Luloff A E, Wang L Y, Xiao J (2016). Impact of land use intensity on sandy desertification: an evidence from Horqin Sandy Land, China. Ecol Indic, 61: 346–358

Geerken R, Ilaiwi M (2004). Assessment of rangeland degradation and development of a strategy for rehabilitation. Remote Sens Environ, 90(4): 490–504

Hao H M, Ren Z Y (2009). Land use/land cover change (LUCC) and eco-environment response to LUCC in farming-pastoral zone, China. Agric Sci China, 8(1): 91–97

Holm A M, Cridland S W, Roderick M L (2003). The use of time-integrated NOAA NDVI data and rainfall to assess landscape degradation in the arid shrubland of Western Australia. Remote Sens Environ, 85(2): 145–158

Huang L, Xiao T, Zhao Z P, Sun C Y, Liu J Y, Shao Q Q, Fan J W, Wang J B (2013). Effects of grassland restoration programs on ecosystems in arid and semiarid China. J Environ Manage, 117: 268–275

Li Q, Zhang C L, Shen Y P, Jia W R, Li J (2016). Quantitative assessment of the relative roles of climate change and human activities in desertification processes on the Qinghai-Tibet Plateau based on net primary productivity. Catena, 147: 789–796

Li S, Zheng Y, Luo P, Wang X, Li H, Lin P (2007). Desertification in western Hainan Island, China (1959 to 2003). Land Degrad Dev, 18 (5): 473–485

Liu F, Zhang H Q, Qin Y W, Dong J W, Xu E Q, Yang Y, Zhang G L, Xiao X M (2016). Semi-natural areas of Tarim Basin in northwest China: Linkage to desertification. Sci Total Environ, 573: 178–188

Lobell D B, Asner G P, Ortiz-Monasterio J I, Benning T L (2003). Remote sensing of regional crop production in the Yaqui Valley, Mexico: estimates and uncertainties. Agric Ecosyst Environ, 94(2): 205–220

Ma G X, Shi M J, Zhao X T, Wang T (2008). Monetary accounting of economic loss of sandy desertification in North China. J Desert Res, 28(4): 627–633 (in Chinese)

Ma Y H, Fan S Y, Zhou L H, Dong Z H, Zhang K C, Feng J M (2007). The temporal change of driving factors during the course of land desertification in arid region of North China: the case of Minqin County. Environ Geol, 51(6): 999–1008

Peters D P C, Havstad K M (2006). Nonlinear dynamics in arid and semi-arid systems: interactions among drivers and processes across scales. J Arid Environ, 65(2): 196–206

Prince S D (2002). Spatial and temporal scales for detection of desertification. In: Reynolds J F, Stafford Smith D M, eds. Global Desertification: Do Humans Cause Deserts? Berlin: Dahlem University Press

Prince S D, Becker-Reshef I, Rishmawi K (2009). Detection and mapping of long-term land degradation using local net production scaling: application to Zimbabwe. Remote Sens Environ, 113(5): 1046–1057

Prince S D, De Colstoun E B, Kravitz L L (1998). Evidence from rain-use efficiencies does not indicate extensive Sahelian desertification. Glob Change Biol, 4(4): 359–374

Prince S D, Wessels K J, Tucker C J, Nicholson S E (2007). Desertification in the Sahel: a reinterpretation of a reinterpretation. Glob Change Biol, 13(7): 1308–1313

Sivakumar M V K (2007). Interactions between climate and desertification. Agric Meteorol, 142(2–4): 143–155

State Forestry Administration of China (2011). The 4th public report of the desertification and sandy desertification in China

State Forestry Administration of China (2015). The 5th public report of the desertification and sandy desertification in China

Sun Y L, Yang Y L, Zhang L, Wang Z L (2015). The relative roles of climate variations and human activities in vegetation change in North China. Phys Chem Earth, 87–88: 67–78

Tan M H, Li X B (2015). Does the Green Great Wall effectively decrease dust storm intensity in China? A study based on NOAA NDVI and weather station data. Land Use Policy, 43: 42–47

Tang Z S, An H, Shangguan Z P (2015). The impact of desertification on carbon and nitrogen storage in the desert steppe ecosystem. Ecol Eng, 84: 92–99

Tao F L, Yokozawa M, Zhang Z, Xu Y L, Hayashi Y (2005). Remote sensing of crop production in China by production efficiency models: models comparisons, estimates and uncertainties. Ecol Modell, 183 (4): 385–396

Tong X W, Wang K L, Yue Y M, Brandt M, Liu B, Zhang C H, Liao C J, Fensholt R (2017). Quantifying the effectiveness of ecological restoration projects on long-term vegetation dynamics in the karst regions of Southwest China. Int J Appl Earth Obs, 54: 105–113

UNCCD (United Nations Convention to Combat Desertification) (1994). United Nations convention to combat desertification in countries experiencing serious drought and/or desertification, particularly in Africa. A/AC, 241/27, Paris

Vu Q M, Le Q B, Vlek P L G (2014). Hotspots of human-induced biomass productivity decline and their social-ecological types toward supporting national policy and local studies on combating land degradation. Global Planet Change, 121: 64–77

Wang F, Pan X B, Wang D F, Shen C Y, Lu Q (2013). Combating desertification in China: past, present and future. Land Use Policy, 31: 311–313

Wang T (2004). Study on sandy desertification in China-3. Key regions for studying and combating sandy desertification. J Desert Res, 24 (1): 1–9 (in Chinese)

Wang T (2014). Aeolian desertification and its control in Northern China. Int Soil Water Conserv Res, 2(4): 34–41

Wang T, Wu W, Xue X, Sun Q W, Chen G T (2004). Study of spatial distribution of sandy desertification in North China in recent 10 years. Sci China Earth Sci, 47(13): 78–88

Wang X M, Chen F H, Dong Z B (2006). The relative role of climatic and human factors in desertification in semiarid China. Glob Environ Change, 16(1): 48–57

Wang X M, Hua T, Lang L L, Ma W Y (2017). Spatial differences of aeolian desertification responses to climate in arid Asia. Global Planet Change, 148: 22–28

Wang X M, Lang L L, Yan P, Wang G T, Li H, Ma W Y, Hua T (2016). Aeolian processes and their effect on sandy desertification of the Qinghai-Tibet Plateau: a wind tunnel experiment. Soil Tillage Res, 158: 67–75

Wang X M, Zhang C X, Hasi E, Dong Z B (2010). Has the Three Norths Forest Shelterbelt Program solved the desertification and dust storm problems in arid and semiarid China? J Arid Environ, 74(1): 13–22

Wessels K J, Prince S D, Frost P E, van Zyl D (2004). Assessing the effects of human-induced land degradation in the former homelands of northern South Africa with a 1 km AVHRR NDVI time-series. Remote Sens Environ, 91(1): 47–67

Wessels K J, Prince S D, Malherbe J, Small J, Frost P E, VanZyl D (2007). Can human-induced land degradation be distinguished from the effects of rainfall variability? A case study in South Africa. J Arid Environ, 68(2): 271–297

Wessels K J, Prince S D, Reshef I (2008). Mapping land degradation by comparison of vegetation production to spatially derived estimates of potential production. J Arid Environ, 72(10): 1940–1949

Wu S H, Yin Y H, Zheng D, Yang Q Y (2005). Aridity/humidity status of land surface in China during the last three decades. Sci China Ser D Earth Sci, 48(9): 1510–1518

Wu Z T, Wu J J, Liu J H, He B, Lei T J, Wang Q F (2013). Increasing terrestrial vegetation activity of ecological restoration program in the Beijing-Tianjin Sand Source Region of China. Ecol Eng, 52: 37–50

Xie X H, Liang S L, Yao Y J, Jia K, Meng S S, Li J (2015). Detection and attribution of changes in hydrological cycle over the Three-North region of China: climate change versus afforestation effect. Agric Meteorol, 203: 74–87

Xu D Y, Kang X W, Liu Z L, Zhuang D F, Pan J J (2009). Assessing the relative role of climate change and human activities in sandy desertification of Ordos region, China. Sci China Earth Sci, 52(6): 855–868

Xu D Y, Li C L, Song X, Re H Y (2014). The dynamics of desertification in the farming-pastoral region of North China over the past 10 years and their relationship to climate change and human activity. Catena, 123: 11–22

Xu D Y, Song A L, Tong H F, Ren H Y, Hu Y F, Shao Q Q (2016). A spatial system dynamic model for regional desertification simulation — A case study of Ordos, China. Environ Model Softw, 83: 179–192

Yan W Z, Hua S (2011). A strategy study on the environmental production of the energy and chemical industry base in northern Shaanxi. Energy Procedia, 5: 969–973

Zhang G L, Dong J W, Xiao X M, Hu Z M, Sheldon S (2012). Effectiveness of ecological restoration projects in Horqin Sandy Land, China based on SPOT-VGT NDVI data. Ecol Eng, 38(1): 20–29

Zhang Y, Zhang C B, Wang Z Q, Chen Y Z, Gang C C, An R, Li J L (2016). Vegetation dynamics and its driving forces from climate change and human activities in the Three-River Source Region, China from 1982 to 2012. Sci Total Environ, 563–564: 210–220

Zhou G S, Zhang X S (1995). A natural vegetation NPP model. Acta Phytoecol Sin, 19(3): 193–200 (in Chinese)

Zhou G S, Zhang X S (1996). Study on NPP of natural vegetation in China under global climate change. Acta Phytoecol Sin, 20(1): 11–19 (in Chinese)

Zhou G S, Zheng Y R, Chen S Q, Luo T X (1998). NPP model of natural vegetation and its application in China. Sci Silva Sin, 34(5): 1–11 (in Chinese)

Zhou W, Gang C C, Zhou F C, Li J L, Dong X G, Zhao C Z (2015). Quantitative assessment of the individual contribution of climate and human factors to desertification in northwest China using net primary productivity as an indicator. Ecol Indic, 48: 560–569